VII International Conference on Computational Methods in Marine Engineering
MARINE 2017
M. Visonneau, P. Queutey and D. Le Touzé (Eds)

AN EXPERIMENTAL STUDY OF THE HYDRODYNAMIC BEHAVIOR OF A TLP PLATFORM FOR A 5MW WIND TURBINE WITH OWC DEVICES

GEORGIOS M. KATSAOUNIS[*], STYLIANOS POLYZOS [*] AND SPYRIDON A. MAVRAKOS[†]

[*] Laboratory for Ship and Marine Hydrodynamics (LSMH)
National Technical University of Athens (NTUA)
9 Heroon Polytechniou str., Zografos GR15773, Athens, Greece
email: katsage@mail.ntua.gr, spolyzos@mail.ntua.gr

[†] Laboratory for Floating Structures and Mooring Systems (LFSMS)
National Technical University of Athens (NTUA)
9 Heroon Polytechniou str., Zografos GR15773, Athens, Greece
email: mavrakos@naval.ntua.gr

Hellenic Center for Marine Research, Director and President
GR19013,Anavyssos, Greece
email: mavrakos@hcmr.gr

Key words: Floating wind turbine, Tension leg platform, Wave energy converter, Oscillating water column, OWC, Wave Tank experiments

Abstract. An experimental study of the hydrodynamic behavior of a Tension-Leg Platform (TLP) for a 5MW Wind Turbine, featuring Wave Energy Converter (WEC) devices of the Oscillating Water Column type is presented. The examined triangular platform includes three vertical cylinders at the corners, providing the required buoyancy, each of them surrounded by a thin skirt, open at its lower end, forming the OWC chamber. A central vertical cylinder is included for the wind turbine installation. All cylinders are structurally connected with cylindrical bracing. The hydrodynamic response of the platform in the surge direction is experimentally verified, together with the resulting pressures and air fluxes inside the OWC chamber and the dynamic tensions in the lines of the mooring system.

1 INTRODUCTION

The development of the offshore wind industry is inevitably linked to the challenge of installation of wind turbines at water depths above the range of 40-70 meters, an area where fixed structures can't be economically installed and operated. For such depths, several designs have been proposed (spar buoys, floaters, semisubmersibles and tension leg platforms), many projects are in the final design stage or in the experimental testing of scaled down prototypes, while there are also some pilot full scale developments [1].

It is evident that the overall cost of a floating installation is increased, as compared against the fixed installations. Thus, any development in the design which results in an augmented harvesting of the available ocean renewable energy has obvious economic advantages. To this end, the combination on a single floating platform of a wind turbine and wave energy converters results in an obvious increase of the captured energy and, also, have both economic and operational advantages [2]. The analysis of the performance of the resulting system requires the simulation of the coupled operation of the wind turbine, the floating platform [3,4] and the OWC device [5,6]. An experimental investigation of the hydrodynamic response of the platform can produce valuable data, useful in the validation of the results of pertinent numerical analyses.

2 FLOATING PLATFORM DESCRIPTION

The examined triangular platform forms a floating basis for the installation of a 5MW NREL offshore wind turbine. The design includes three vertical cylinders at the corners, providing the required buoyancy. Each of them is surrounded by a thin skirt, open at its lower end, forming the OWC chamber. A central vertical cylinder is included in the arrangement for the installation of the wind turbine. All cylinders of the hull of the platform are structurally connected and supported by cylindrical bracing. The design is shown schematically in the following graph, where the domes of the OWC chambers have been removed to give access to the cylinders.

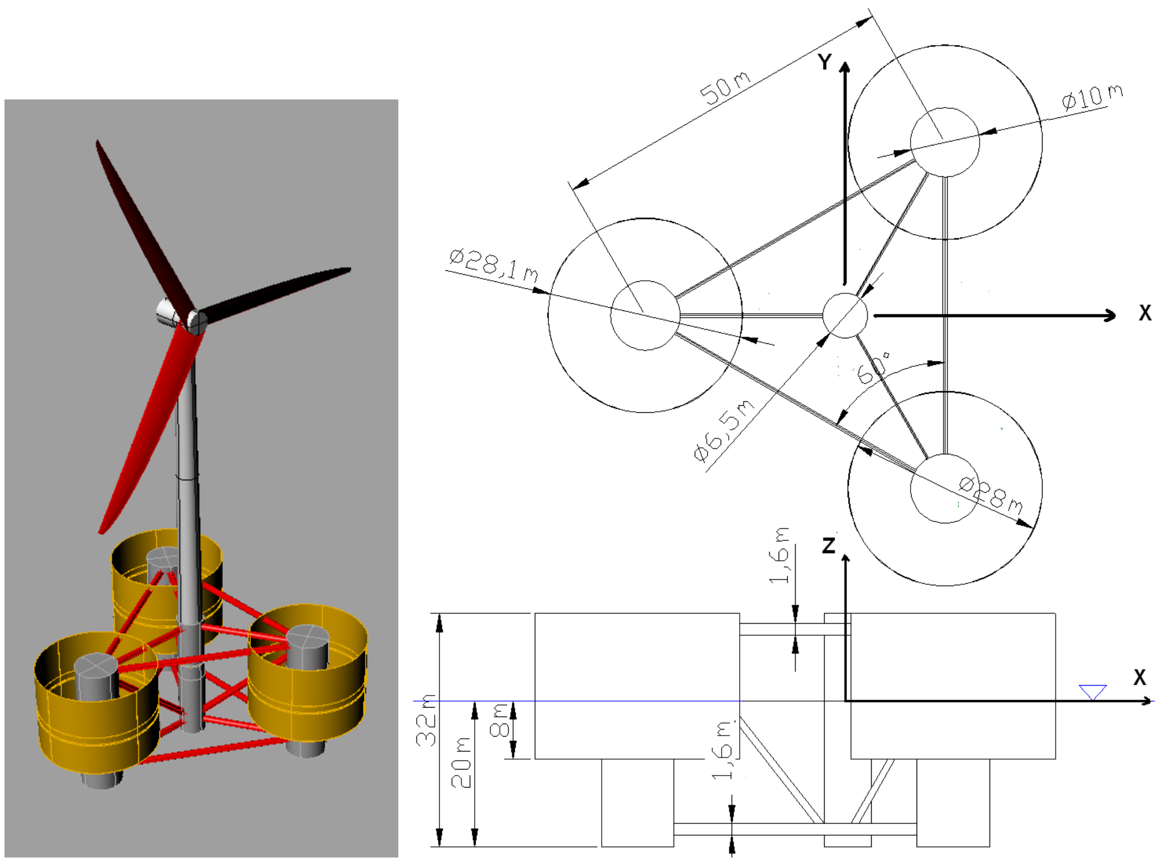

Figure 1: TLP platform dimensions

The mooring of the platform follows the tension leg concept. Three wire legs connect the bottom of the corner cylinders to the sea bed foundation, providing also the required pretension for the stabilization of the platform and for station keeping.

The weight groups of the platform and the tendon characteristics are summarised in the following table:

Table 1: Platform particulars

Platform mass	2183 t
Wind turbine and tower	600 t
Displacement	6.086,3 t
Vertical center of gravity of the platform (below sea level)	4,05m
Nominal Tendon pretension (each)	10.800kN
Tendon diameter	239mm
Water depth	120m

Under the action of the incident waves, the water contained between each cylinder and the corresponding skirt, acts as an oscillating water column and the resulting flux of air can be converted into electric energy by means of an air turbine. The hydrodynamic behavior of such an arrangement is quite complex, since the incident waves, the mooring, the motion of the platform, the behavior of the water column and the effect of the air turbine, are all interrelated and affect the ability of the system to convert wave energy into electricity.

In order to examine the behavior of such a system, an extensive set of experiments on a scaled down model of the platform (scale 1:40), were conducted in the wave tank of the Laboratory for Ship and Marine Hydrodynamics (LSMH) of the National Technical University of Athens (NTUA). The Froude scaling law was followed for the modelling of the wave environment. In the following paragraphs, the experimental setup and instrumentation is discussed, along with the modeling for the wind turbine and the wave energy converter.

Experiments were conducted for a wide range of incident waves, both harmonic and irregular, corresponding to the sea-states a TLP is expected to encounter in the Aegean Sea. In this work, the results of the above experimental study will be presented, in terms of the TLP motions in the surge x-direction under the action of harmonic waves, the loads on the mooring tendons, the wind turbine tower loads at its mounting location on the floating platform and the flow characteristics (flux and pressure) inside the WEC devices.

3 MEASURING SYSTEM

The response of the platform subjected to the wave action was recorded by an optical system. An array of four digital cameras was arranged at the side of the wave tank, to record the motion of special optical targets placed at various locations on the platform and on the tower of the wind turbine. The recorded frames were then analysed by optical recognition software, providing time histories of the motion.

The amplitudes of the waves generated by the wave maker of the tank were measured by two standard wave probes of wire type, one located near the wave maker while the other located in front of the platform. For the measurement of the internal water surface inside the

OWC device, three wave probes were used, located radially in the toroidal space of the OWC air chamber, spaced 120^o apart. The elevation of the internal surface was obtained on the basis of these elevation measurements, assuming a flat shape for the internal surface and considering also that the motions of the TLP platform are mainly horizontal, due to the large amount of the pretension of the TLP system. The air volume flux was then computed by time differentiating the above measurements, taking into account the area of the OWC net cross section. All signals were sampled at a rate of 100Hz and subjected subsequently in digital filtering and recording.

The time histories of the pressures inside the air chamber of the OWC device were measured by three pressure transducers, two of them located on the dome of the chamber of the front cylinder, while the third sensing the outside pressure.

For the measurement of the exerted loads on the base of the tower of the wind turbine a 6-dof load cell was inserted, between the tower base and the platform. Furthermore, the accelerations of the platform were captured by accelerometers installed on the platform deck and along the wind turbine tower.

For the modeling of the static thrust of the wind turbine, two small thrusters were installed at the nacelle level and were calibrated to produce the required thrust.

Finally, three underwater load cells were inserted in the tendon lines, at their bottom end, for the measurement of the static pretension and dynamic tension of the mooring legs.

4 NATURAL FREQUENCIES IN SURGE MOTION

4.1 Stiffness in surge motion

The stiffness provided by the pretension or the tendons of the mooring system was measured by imposing specific loads along the surge –x direction and measuring the resulting offset of the platform. In this way, a value of 214 N/m was obtained, which corresponds to 342,4 kN/m for the full scale configuration.

4.2 Natural frequencies and damping coefficient

Free decay tests were carried out for the measurement of the natural frequency of the platform in surge motion. An initial displacement was imposed along the surge degree of freedom and the platform was then released to perform free decaying oscillations. A time history, representative of the decaying oscillations, is presented in figure 2. The measurements were analyzed in order to obtain the natural frequency and the damping parameter of the oscillation. The results for the frequency are summarized in Table 2, where it is shown that the surge natural frequency is 0.864 rad/sec (model scale), corresponding to 0.137 rad/sec in full scale.

The critical damping ratio in surge motion, as calculated on the basis of the logarithmic amplitude decay of the time histories, is presented in figure 3 (model scale), plotted against the amplitude of the oscillation. An increasing trend of the damping ratio with respect to the amplitude of oscillation can be concluded. For infinitesimal amplitudes the critical damping ration is obtained as 0.0307 for the model scale.

Table 2: Frequencies of free surge oscillations

Initial Offset	Period [sec] Model scale	Freq. [rad/sec] Model scale	Freq. [rad/sec] Full scale
27	7.10	0.885	0.140
50	7.29	0.862	0.136
74	7.30	0.861	0.136
120	7.34	0.856	0.135
119	7.33	0.857	0.136
Average	7.27	0.864	0.137

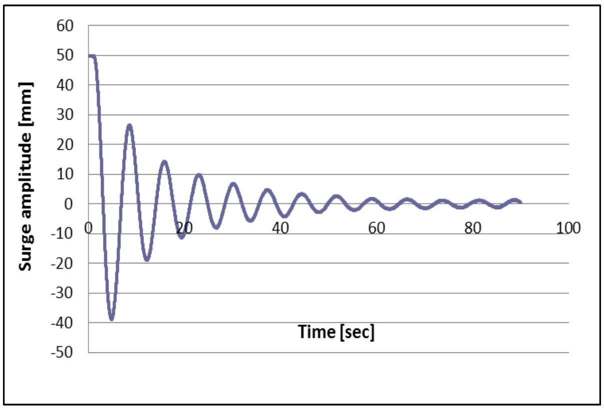

Figure 2: Surge free oscillation (model)

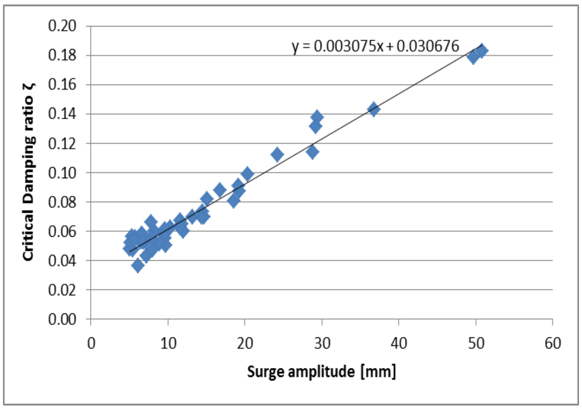

Figure 3: Critical damping ratio (model)

5 HYDRODYNAMIC RESPONSE

The platform was subjected to the action of harmonic wave trains, produced by the wave maker of the basin. The calculated non dimensional linear response amplitude operators (RAOs) for the surge motion of the platform are presented in figure 4.

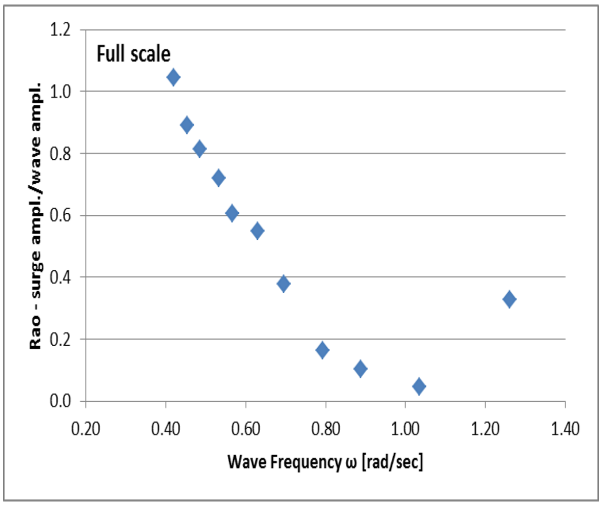

Figure 4: Surge motion Raos

Figure 5 present the response operators for the induced accelerations at the base of the tower of the wind turbine, while figure 6 depicts the corresponding coefficients for the bending moments at the same location. A peak of the above responses in the vicinity of 1.27 Hz (1.26 rad/sec full scale) is remarkable. This may result in a heavy loading of the tower of the air turbine, affecting also the fatigue strength of the structure.

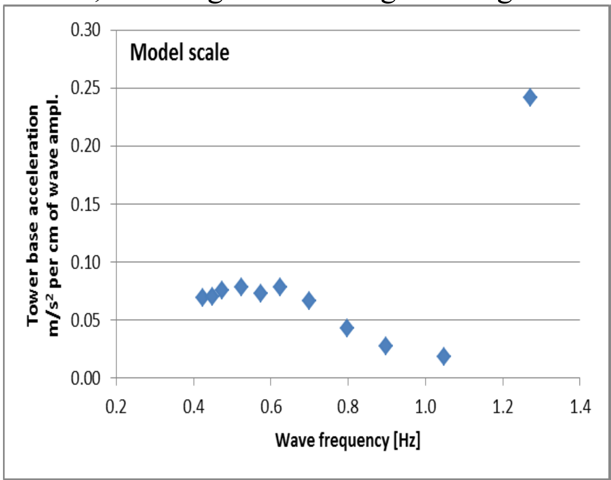

Figure 5: Linear acceleration at tower base

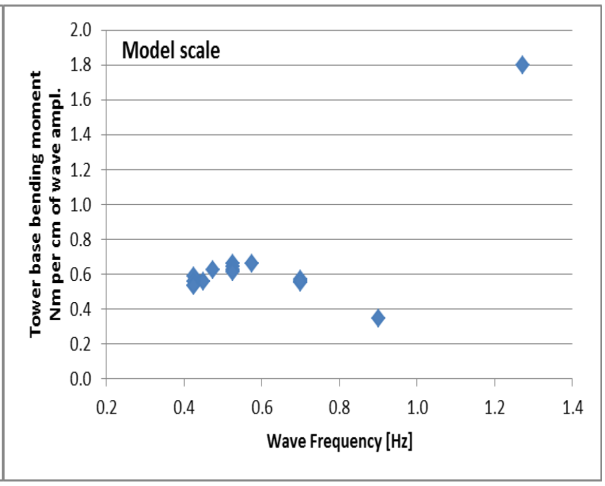

Figure 6: Bending moments at tower base

6 MEASUREMENTS OF THE OWC PARAMETERS

The parameters that are relevant to the performance of the OWC device are the pressure difference (drop) between the air chamber and the outside space and the volumetric flow rate, passing through the air turbine of the device. Usually, a Wells turbine is used to convert the energy of the air flow to electricity. This is a bidirectional device, designed for directional changing air flows, like the ones produced in the air chamber of the OWC under the action of the oscillating water surface, due to the wave action. The integration of a scaled down model of a Wells air turbine in the presented model of the TLP platform was outside the scope of the work presented herein. Thus, an equivalent model for the simulation of the effect of the turbine on the air flow was necessary. For this purpose, an orifice (small diaphragm with a hole) was formed at the top of the conical domes of the OWC air champers. Tests were carried out with the orifice hole having several diameters, namely 20, 40 and 50mm, since the effect of the orifice on the pressure depends on the value of the diameter. In general, the effect of a Wells turbine is approximated, in pertinent numerical models, by a linearised relationship between the pressure drop and the corresponding volumetric flow rate:

$$\Delta p = \Lambda Q \tag{1}$$

Where Δp is the pressure drop, Q the volumetric flow rate of the air, assumed incompressible, and Λ a device parameter, depended generally on the diameter, the rotational speed, and the specific particulars of the air turbine. The selection of the Λ value obviously affects the operation of the device, thus it should be subjected to optimization. Such a procedure is outside the scope of the presented work, as already mentioned, since no scaled down model of the air turbine was available. Following the approach with the orifice usage, an equivalent linearized relationship between pressure drop and volumetric flow rate can be established, by linearising the nonlinear relation, pertinent to the orifice action. Indeed, the volumetric flow rate is related to the pressure drop by a general equation in the form of:

$$Q = C_f A_0 \sqrt{(\Delta p/\rho)} \tag{2}$$

where ρ the air density A_0 the orifice area and C_f the orifice parameter, usually defined experimentally. Solving for Δp it can be obtained:

$$\Delta p = \frac{1}{2}\rho \frac{1}{c_f^2 A_0^2} Q^2 \tag{3}$$

and, by considering bidirectional flows:

$$\Delta p = C_e\, Q\, |Q| \tag{4}$$

where C_e an equivalent coefficient, to be determined experimentally.
In the presented experimental work the instantaneous pressure drops was measured by the pressure transducers of the measuring system, while the volumetric flow rates were computed on the basis of the wave probe readings inside the air chamber. In the following figure the instantaneous pressures are plotted against the volumetric flow rates, in order to obtain the C_e values. Many individual curves are over-plotted in the figure, obtained from many experiments, with various wave amplitudes. The nonlinear character of the relation between the pressure and the flow rate is evident. However, an equivalent linearization can in principle be obtained, by defining a linear regression on a specific range of the pressures, or flows, of interest.

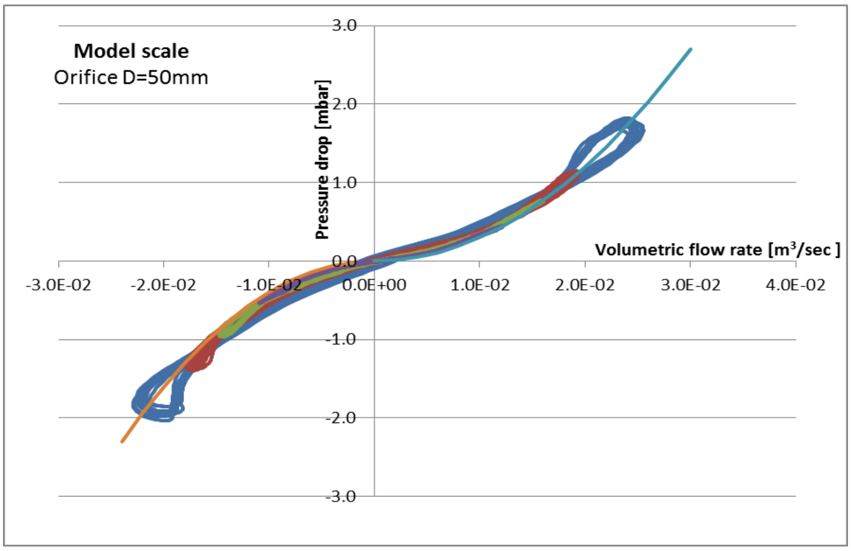

Figure 7: Pressure drop to flow rate relation

An approximate curve can be fitted to the above experimental data:

Orifice diameter 50mm, Flow rates up to 0.026 m^3/sec:

Compression phase: $\Delta p = 3\ 10^3\ Q\ |Q|$ $\quad$ Δp[mbar], Q[m^3/sec] (5)

Suction phase: $\Delta p = 4\ 10^3\ Q\ |Q|$

Similar curves were obtained also for the orifice diameters of 40 and 20mm, resulting in the following estimations:

Orifice diameter 40mm, Flow rates up to 0.025 m^3/sec:

$$\text{Compression phase: } \Delta p = 7\ 10^3\ Q\ |Q| \qquad \Delta p[mbar],\ Q[m^3/sec] \tag{6}$$

$$\text{Suction phase: } \Delta p = 8\ 10^3\ Q\ |Q|$$

Orifice diameter 20mm, Flow rates up to 0.006 m^3/sec:

$$\text{Compression phase: } \Delta p = 100\ 10^3\ Q\ |Q| \qquad \Delta p[mbar],\ Q[m3/sec] \tag{7}$$

$$\text{Suction phase: } \Delta p = 80\ 10^3\ Q\ |Q|$$

The pressure drops in the front cylinder, plotted against the frequency of the incoming waves, are shown in the following figures. The values are given as linearised RAO's and were based on tests with harmonic waves having various amplitudes. A scattering of the values can be observed, maybe due to the aforementioned nonlinear character of the orifice equation, which affects the pressure formation.

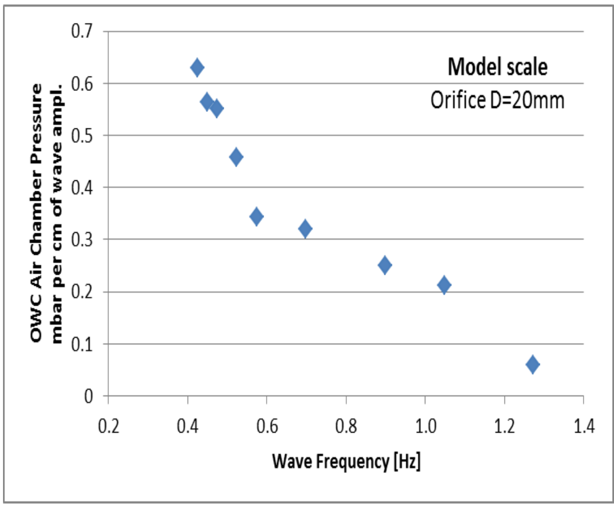

Figure 8: OWC chamber pressures, Orifice D=20mm

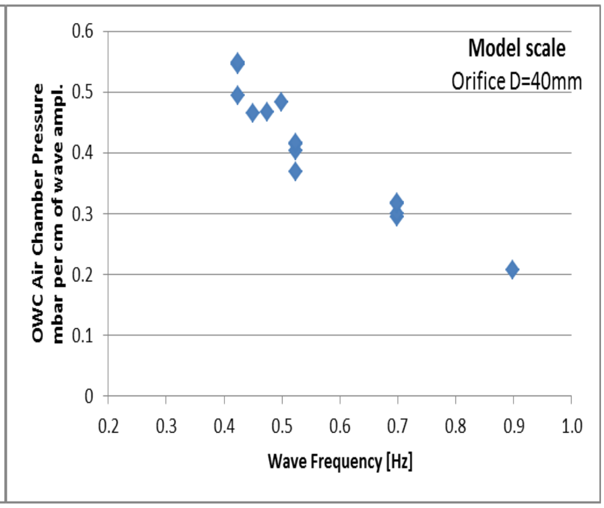

Figure 9: OWC chamber pressures, Orifice D=40mm

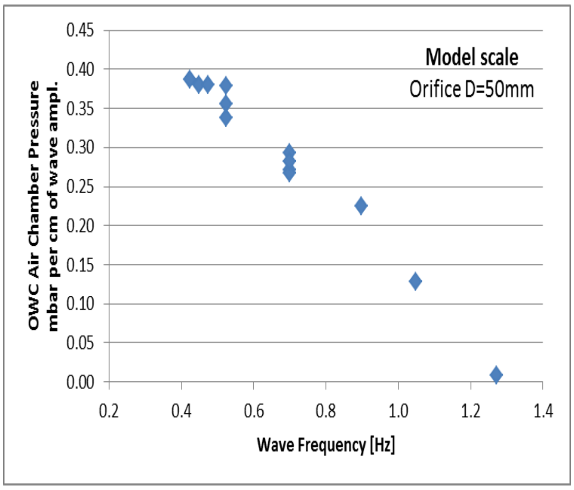

Figure 10: OWC chamber pressures, Orifice D=50mm

7 DYNAMIC TENSION ON THE MOORING LINES

The dynamic tension exerted on the mooring lines of the TLP platform seems dominated by the pressure formation inside the chambers of the OWC devices. The following figures present the dynamic tension of the mooring line of the front cylinder, as linearised RAO's. The same observation regarding the scatter of the values can also be made here, like in the case of the pressure drop.

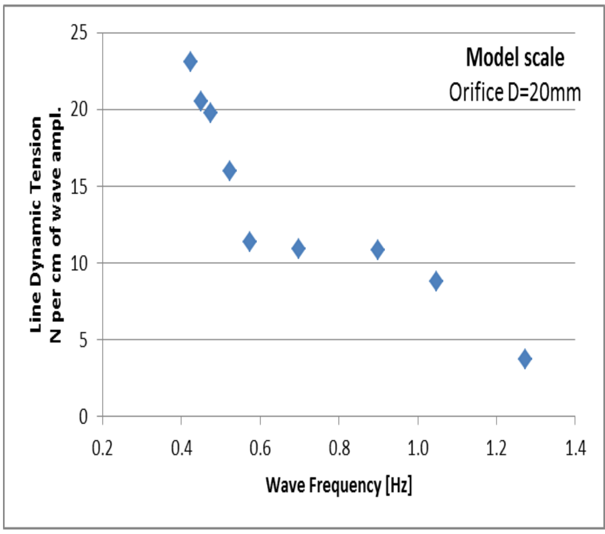

Figure 11: Tendon dynamic tension, Orif. D=20mm

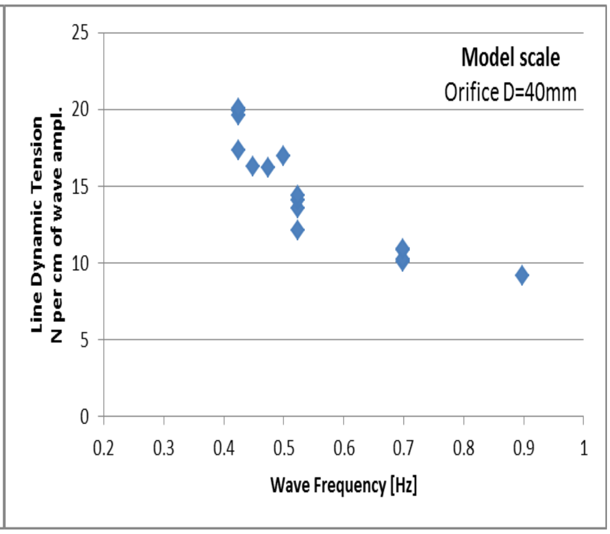

Figure 12: Tendon dynamic tension, Orif. D=40mm

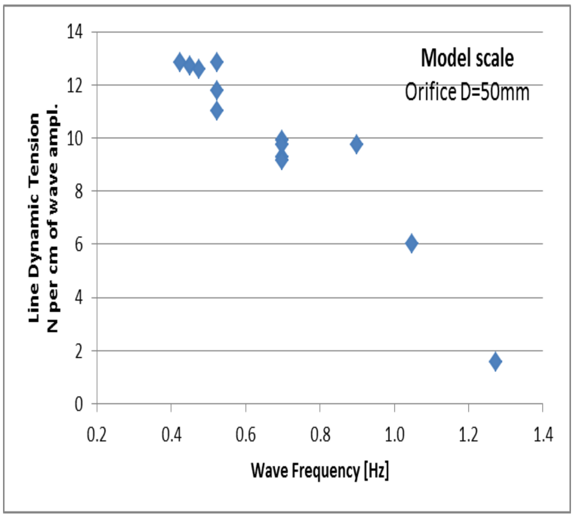

Figure 13: Tendon dynamic tension, Orif. D=50mm

12 CONCLUSIONS

- An experimental study of the hydrodynamic behaviour of a TLP platform for the installation of a 5MW NREL wind turbine and three OWC devices is presented.
- Data for the natural frequency in surge motion and response amplitude operators for

surge motion, pressures inside the OWC chamber and dynamic tensions in the tendons were experimentally obtained.

- The relation between the chamber pressure and the volumetric flow rate in the OWC chamber was presented for several simulations of the effect of the air turbine, through the use of an orifice device.
- The presented data can be useful in the validation of the results of numerical simulations of motion and performance of this complex system.

REFERENCES

[1] Bossler, A., Floating offshore wind foundations: industry projects in the USA, Europe and Japan, *Technical Report* (2013), Maine International Consulting, Inc.

[2] Aubault, A., Alves, M., Sarmento, A., Roddier D. and Peiffer, A., Modeling of an Oscillating Water Column on the Floating Foundation Windfloat, *Proc. of the ASME 30th International Conference on Ocean, Offshore and Arctic Engineering*, OMAE2011-49014, (2011).

[3] Sclavounos, P., Floating offshore wind turbines, *Marine Technology Society Journal*, (2008), 42, 39-43.

[4] Jonkman, J. M., Dynamics Modeling and Loads Analysis of an Offshore Floating Wind Turbine, *Technical Report*, (2007) NREL/TP-500-41958, National Renewable Energy Lab, Golden, Colorado.

[5] Evans D.V., Wave-power Absorption by Systems of Oscillating Surface Pressure Distributions, *Journal of Fluid Mechanics*, (1982), Vol. 114, p. 481–499.

[6] Konispoliatis, D.N., Mavrakos, S.A., Hydrodynamic Analysis of an Array of Interacting Free-Floating Oscillating Water Column (OWC's) Devices, *Ocean Engineering* (2016) 111, p. 179–197.